Supporting Information

A new dithieno[3,2-b:2',3'-d]thiophene derivative for high performance single crystal organic field-effect transistors and UV-sensitive phototransistors

Yunpeng Lou, [a] Rui Shi, [a] Li Yu, [a] Ting Jiang, [a] Haoquan Zhang, [a] Lifeng Zhang, [d] Yongxu Hu, [a] Deyang Ji, [a] Yajing Sun,*[b] Jie Li,*[a] Liqiang Li [ac] and Wenping Hu [bc]

[a] Tianjin Key Laboratory of Molecular Optoelectronic Sciences, Department of Chemistry, Institute of Molecular Aggregation Science, Tianjin University, Tianjin 300072, China. E-mail: syg19@tju.edu.cn, lijie2018@tju.edu.cn.

[b] Tianjin Key Laboratory of Molecular Optoelectronic Sciences, Department of Chemistry, School of Science, Tianjin University, Tianjin 300072, China.

[c] Joint School of National University of Singapore and Tianjin University, International Campus of Tianjin University, Binhai New City, Fuzhou 350207, China.

[d] Institute of Molecular Plus, Tianjin University, Tianjin 300072, China.

Table of contents

1. General Information..S1

2. Synthesis...S2

3. Optical properties...S2

4. Thermal stability of 2,6-DADTT...S3

5. Ultraviolet photo-electron spectroscopy...S4

6. Crystal structures..S4

7. Characterizations of 2,6-DADTT single crystals...S7

8. Characterization of 2,6-DADTT-based SC-OFETs...S8

9. Characterization of 2,6-DADTT-based single crystal phototransistors................S10

10. MALDI-TOF MS...S12

11. Summary of the figures of merits of the UV-sensitive OPTs reported.............S13

12. References..S14

1. General Information

1.1 Materials and instruments

The materials and reagents we used were commercially available and used without any further purification. Thermogravimetric analysis (TGA) was measured from 50 °C to 700 °C by Thermo Gravimetric Analyzer TG 209F3 with a scanning rate of 10 °C/min in N_2. UV-vis absorption spectra were obtained from Shimadzu UV-3600 UV-vis spectrophotometer. Photoluminescence (PL) spectra were recorded on FLS1000 fluorescence spectrophotometer. X-ray diffractometer data was recorded on MiniFlex600 (Rigaku). X-ray crystallography data were collected on XtaLAB Fr-X X-ray single-crystal diffractometer. Atomic force microscopy (AFM) were carried out with Digital Instruments Nano-scope III atomic force microscope in air. Transmission electron microscopy (TEM) and selected area electron diffraction (SAED) were conducted on Thermo Scientific Talos F200X. Ultraviolet photoelectron spectroscopy (UPS) (KRATOS Axis Ultra DLD spectrometer) measurements were taken with He I (h = 21.22 eV) as the excitation source under a base pressure > 2 × 10^{-9} torr. The single crystals of 2,6-DADTT were prepared by vacuum sublimation in BTF-1200°C vacuum tube furnace. Energy-minimized models of 2,6-DADTT were calculated by Gaussian 09W program at the B3LYP/6-31G(d, p) level of Density Function Theory (DFT). The transfer integrals were calculated by MOMAP program. [1]

1.2 Device fabrication and characterization

In order to reduce the residue hydroxy on Si/SiO_2 substrate, the octadecyl-trichlorosilane (OTS) was modified on Si/SiO_2 substrate following the steps: (1) The Si/SiO_2 wafers containing 300 nm-thick SiO_2 layer were treated with O_2 plasma (5 minutes, 50 W). (2) The substrates and OTS (10 µL) were heated in the vacuum oven at 120 °C for two hours. (3) After cooling to room temperature, the substrates were ultrasonically cleaned with n-hexane, chloroform, isopropanol for 10 minutes, respectively. (4) The substrates were dried with a flow of high-purity nitrogen. After modifying the substrates, the single crystals were prepared by the physical vapor transport (PVT) method with high-purity nitrogen. High-quality 2,6-DADTT single crystals were obtained at 297 °C with 100 sccm gas flow rate for 180 min. Finally, the gold as source and drain electrodes was laminated on the crystal by "gold stamp method" that could avoid the thermal radiation, and the channel width (W) and channel length (L) of the devices were measured by the Optical Microscope. The electrical characteristics of these devices were tested by an Agilent B1500A semiconductor parameter analyzer. The charge carrier mobility in the saturated region was calculated according to $I_{DS} = \left(\frac{W}{2L}\right) C_i \mu (V_G - V_T)^2$. The photo response behaviors were tested under the irradiation of fixed wavelength laser (365 nm).

To evaluate the performance of 2,6-DADTT single crystal phototransistors, photosensitivity (P), responsivity (R) and detectivity (D*) were calculated according to the following equations:

$$P = |I_{photo}-I_{dark}| / I_{dark} \quad (1)$$

$$R = |I_{photo}-I_{dark}| / SP_i \quad (2)$$

$$D^* = RS^{1/2}/(2eI_{dark})^{1/2} \quad (3)$$

I_{photo} and I_{dark} are the drain current under illumination and dark, respectively. S is the illuminated channel area and P_i is the incident light intensity.

2. Synthesis of 2,6-DADTT

2,6-dibromodithieno[3,2-b:2',3'-d]thiophene (0.354 g, 1 mmol), anthracen-2-ylboronic acid (0.532 g, 2.4 mmol) , Tetrakis(triphenylphosphine)palladium(0) (0.096 g , 0.08 mmol) and Potassium carbonate (0.552 g, 4 mmol) were added to a 10 ml reaction bottle , and then dissolved in mixed solvent (6 mL) including toluene, EtOH and H_2O (4 : 1 : 1, volume ratio) , under nitrogen atmosphere. The mixed solution was stirred at 100 °C for 24 h. After reaction stopped and cooled down to room temperature, the mixture was filtered and then washed by dichloromethane, water and ethanol, and finally dried by the oven under vacuum to obtain the crude product (0.42 g). The production yield for the crude product was 76.7%. Subsequently, it was purified by sublimation under high vacuum at 280 °C. The production yield was 31.5% after first sublimation. MS (MALDI-TOF): calculated for $C_{36}H_{20}S_3$: 548.07, found: 548.07203.

3. Optical properties

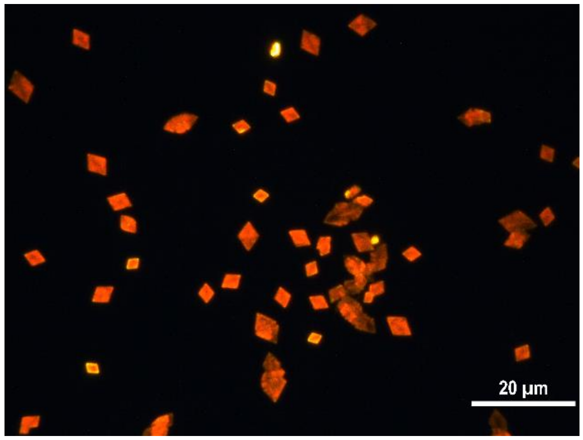

Fig. S1 Fluorescence image of 2,6-DADTT single crystals under UV light irradiation.

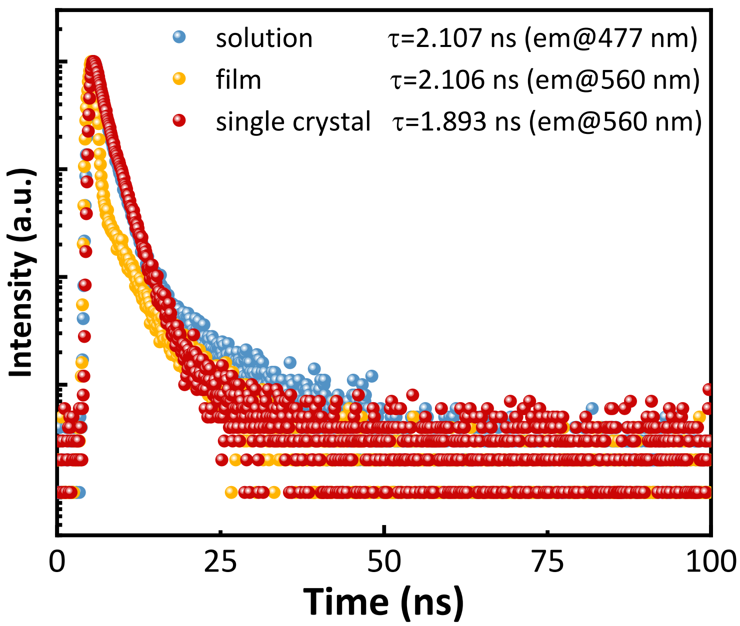

Fig. S2 Fluorescence lifetime of 2,6-DADTT.

Table S1. Absorption and fluorescence data of 2,6-DADTT.

	State	$\lambda_{abs.}$ (nm)	$\lambda_{em.}$ (nm)	Φ (%)
2,6-DADTT	solution	210,237,290,324,362,382,405	477	34.76
	film	338,367,400,426	560,608	/
	crystal	260,362,397,420	560,604	/

4. Thermal stability of 2,6-DADTT.

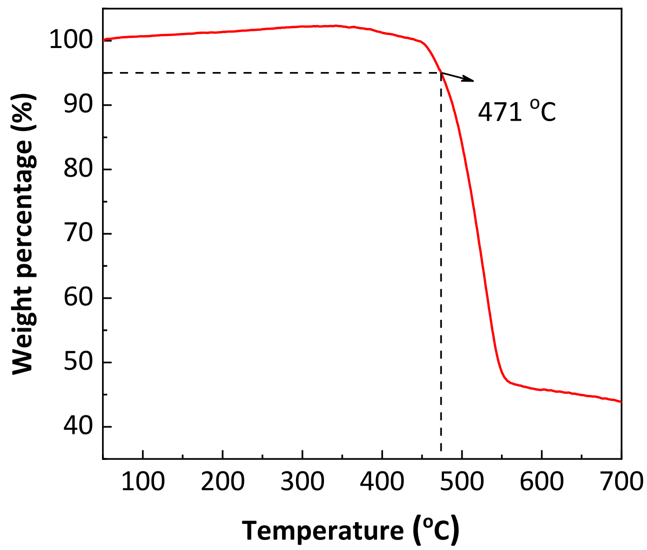

Fig. S3 Thermal gravimetric analysis (TGA) of 2,6-DADTT.

5. Ultraviolet photo-electron spectroscopy.

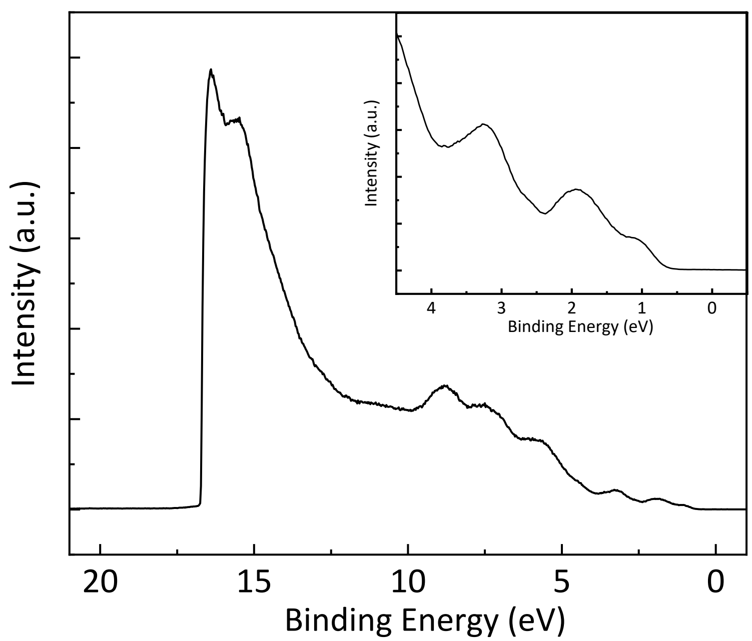

Fig. S4 UPS energy distribution curve of 2,6-DADTT.

6. Crystal structures.

Table S2. Crystal Data of 2,6-DADTT (CCDC: 2237416).

	2,6-DADTT
Empirical Formula	C36H20S3
Formula Weight	548.74
Temperature/K	160 K
Wavelength/Å	1.54184
Crystal System	monoclinic
Space group	P 21/c
a/Å	7.4830(3)
b/Å	5.9649(2)
c/Å	55.0355(14)
α	90
β	101.485(3)
γ	90
Volume/Å3	2407.34
Z	4
F (000)	1136.0
Theta range for data collection	3.276 to 149.73
Index ranges	-9 ≤ h ≤ 9, -6 ≤ k ≤ 7, -66 ≤ l ≤ 67
Reflections collected	71967
Independent reflections	4784 [Rint = 0.1780, Rsigma = 0.0732]
Good-of-fit on F2	1.043
Final R indexes [I>=2σ (I)]	R1 = 0.0679, wR2 = 0.1344
Final R indexes [all data]	R1 = 0.1216, wR2 = 0.1611

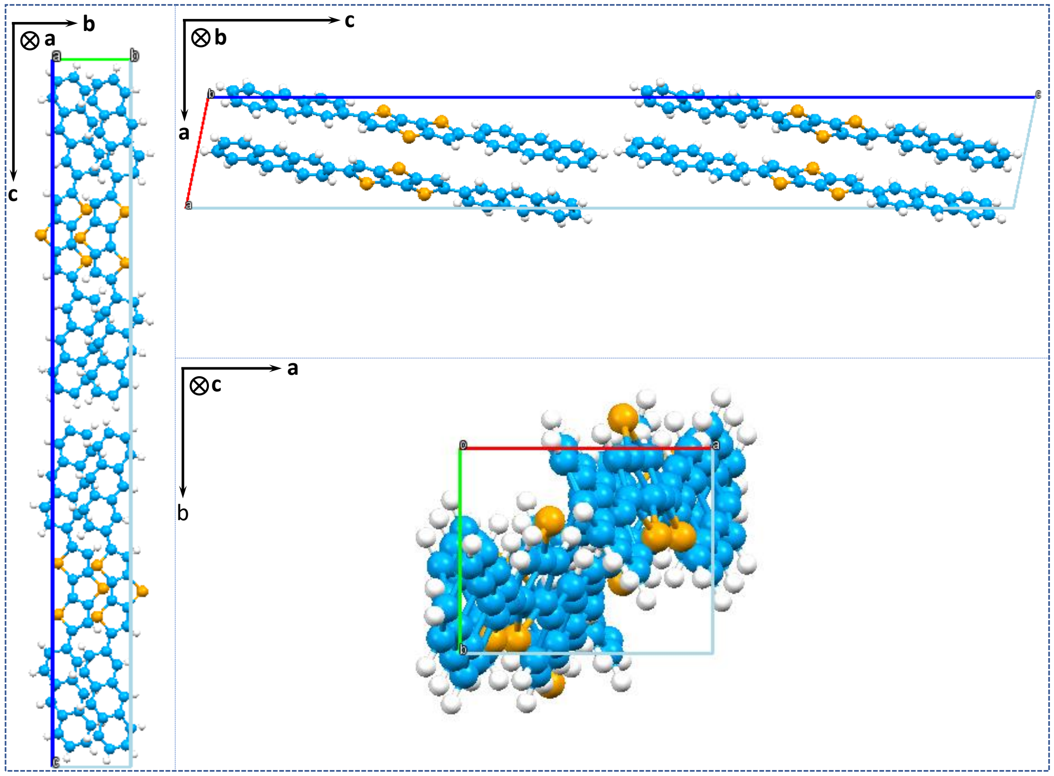

Fig. S5 The molecular packing of 2,6-DADTT molecules along different axis.

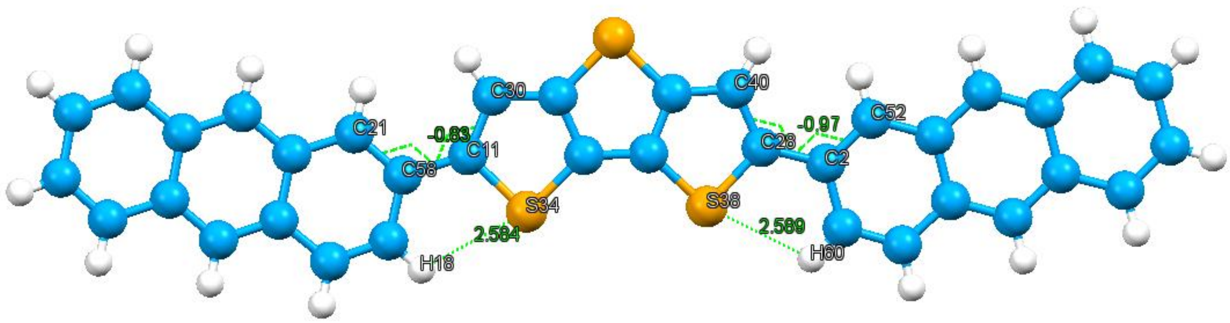

Fig. S6 Measurement of torsion angle between the dithieno[3,2-b:2′,3′-d]thiophene core and the anthracene group and distance of the intramolecular S···H interaction.

7. Characterizations of 2,6-DADTT single crystals.

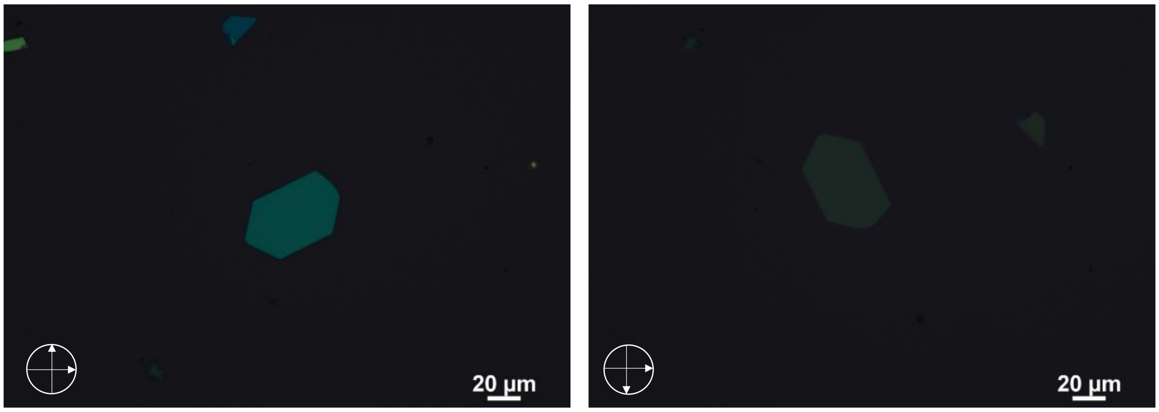

Fig. S7 Polarized optical microscope of an individual 2,6-DADTT single crystal.

8. Characterization of 2,6-DADTT-based SC-OFETs.

Table S3. Comprehensive performances of 2,6-DADTT-based SC-OFETs.

	μ_{max} ($cm^2 V^{-1} s^{-1}$)	μ_{ave} ($cm^2 V^{-1} s^{-1}$)	I_{on}/I_{off}	V_{th} (V)
2,6-DADTT	1.26	0.706	10^6 - 10^8	-15.46-22.39

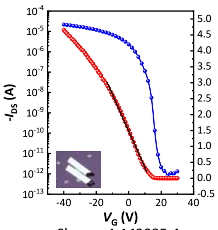

Slope =-1.14208E-4,
Intercept =0.00149,
μ = 0.458 $cm^2 V^{-1} s^{-1}$,
V_{th} = 13.05 V
I_{on}/I_{off} = 1.88X 10^7
W/L = 57/11

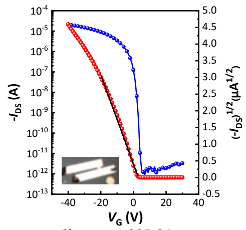

Slope = -1.32E-04,
Intercept =4.53E-04,
μ = 1.26 $cm^2 V^{-1} s^{-1}$,
V_{th} = 3.42V
I_{on}/I_{off} = 1.72 X 10^7
W/L = 43/17

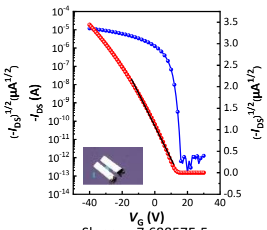

Slope = -7.68857E-5,
Intercept = 0.00109,
μ = 0.842 $cm^2 V^{-1} s^{-1}$,
V_{th} = -14.18 V
I_{on}/I_{off} = 1.85 X 10^7
W/L = 60/47

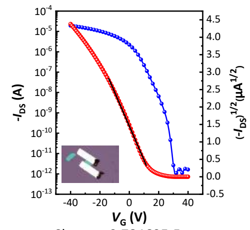

Slope = -9.78469E-5
Intercept = 0.00146,
μ = 0.826 $cm^2 V^{-1} s^{-1}$,
V_{th} = -14.92 V
I_{on}/I_{off} = 1.76 X 10^7
W/L = 99/47

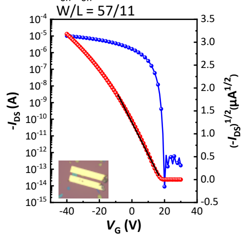

Slope =-7.07E-05,
Intercept =1.27E-03,
μ = 0.454 $cm^2 V^{-1} s^{-1}$,
V_{th} = 17.96 V
I_{on}/I_{off} = 1.12 X 10^8
W/L = 2

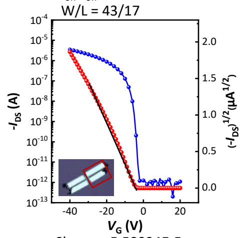

Slope = -5.58834E-5
Intercept = -1.99209E-4,
μ = 0.879 $cm^2 V^{-1} s^{-1}$,
V_{th} = -3.56 V
I_{on}/I_{off} = 2.91 X 10^6
W/L = 31/48

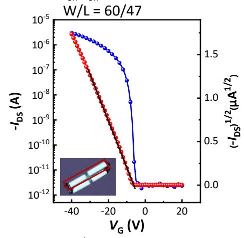

Slope = -5.34214E-5
Intercept = -3.25758E-4,
μ = 0.685 $cm^2 V^{-1} s^{-1}$,
V_{th} = -6.10 V
I_{on}/I_{off} = 1.01 X 10^6
W/L = 53/70

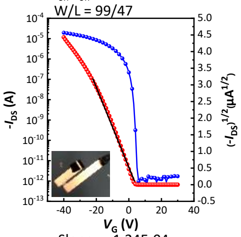

Slope = -1.24E-04,
Intercept =5.18E-04,
μ = 1.25 $cm^2 V^{-1} s^{-1}$,
V_{th} = 4.18V
I_{on}/I_{off} = 2.01 X 10^7
W/L = 49/22

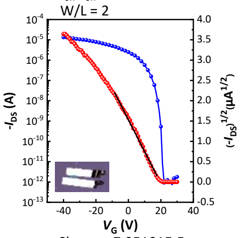

Slope = -7.95101E-5,
Intercept = 0.00155,
μ = 0.511 $cm^2 V^{-1} s^{-1}$,
V_{th} = 19.49 V
I_{on}/I_{off} = 1.06 X 10^7
W/L = 9/4

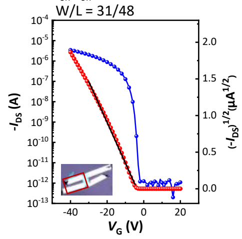

Slope = -5.54293E-5
Intercept = -1.93306E-4,
μ = 0.958 $cm^2 V^{-1} s^{-1}$,
V_{th} = -15.46V
I_{on}/I_{off} = 2.82 X 10^6
W/L = 59/70

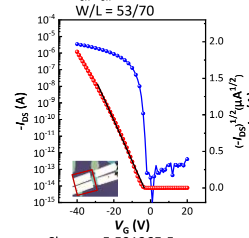

Slope = -5.59136E-5,
Intercept =-1.99341E-4,
μ = 0.853 $cm^2 V^{-1} s^{-1}$,
V_{th} = -3.57 V
I_{on}/I_{off} = 2.07 X 10^7
W/L = 2/3

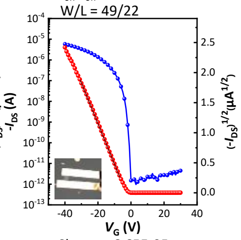

Slope = -6.65E-05,
Intercept =-1.62E-04,
μ = 0.82 $cm^2 V^{-1} s^{-1}$,
V_{th} = -2.43V
I_{on}/I_{off} = 3.9 X 10^6
W/L = 61/62

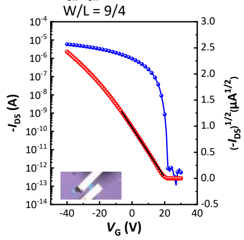

Slope = -4.85018E-5,
Intercept = 9.77807E-4,
μ = 0.371 $cm^2 V^{-1} s^{-1}$,
V_{th} = 1.00 V
I_{on}/I_{off} = 5.84 X 10^6
W/L = 15/13

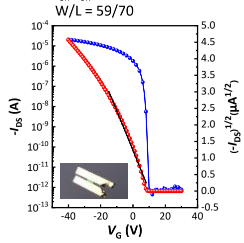

Slope = -1.20473E-4,
Intercept = 0.00124,
μ = 0.505 $cm^2 V^{-1} s^{-1}$,
V_{th} = 10.29 V
I_{on}/I_{off} = 1.92 X 10^7
W/L = 115/22

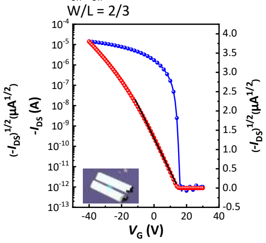

Slope = -8.54873E-5,
Intercept = 0.00128,
μ = 0.633 $cm^2 V^{-1} s^{-1}$,
V_{th} = 14.97V
I_{on}/I_{off} = 1.41 X 10^7
W/L = 21/10

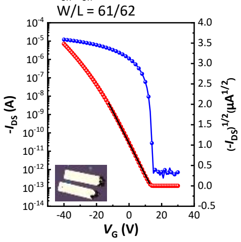

Slope = -7.88781E-5,
Intercept = 0.00105,
μ = 0.620 $cm^2 V^{-1} s^{-1}$,
V_{th} = 13.31V
I_{on}/I_{off} = 1.23 X 10^7
W/L = 73/40

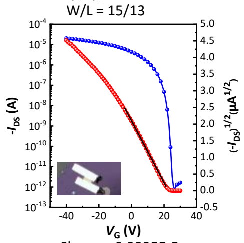

Slope = -9.3325E-5
Intercept = 0.00209,
μ = 0.412 $cm^2 V^{-1} s^{-1}$,
V_{th} = 22.39 V
I_{on}/I_{off} = 1.24 X 10^7
W/L = 134/35

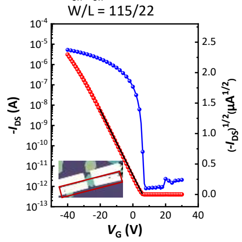

Slope = -5.44682E-5,
Intercept = 2.87526E-4,
μ = 0.772 $cm^2 V^{-1} s^{-1}$,
V_{th} = 5.28 V
I_{on}/I_{off} = 4.41 X 10^6
W/L = 65/93

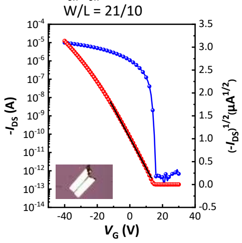

Slope = -6.66263E-5,
Intercept = 0.00103,
μ = 0.499 $cm^2 V^{-1} s^{-1}$,
V_{th} = 15.46 V
I_{on}/I_{off} = 1.49 X 10^7
W/L = 55/34

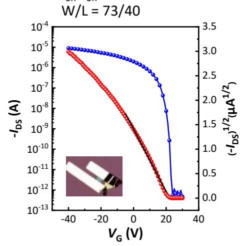

Slope = -6.38526E-5,
Intercept = 0.00141,
μ = 0.516 $cm^2 V^{-1} s^{-1}$,
V_{th} = 22.08 V
I_{on}/I_{off} = 7.83 X 10^6
W/L = 23/16

Fig. S8 Transfer curves of twenty SC-OFETs based on 2,6-DADTT.

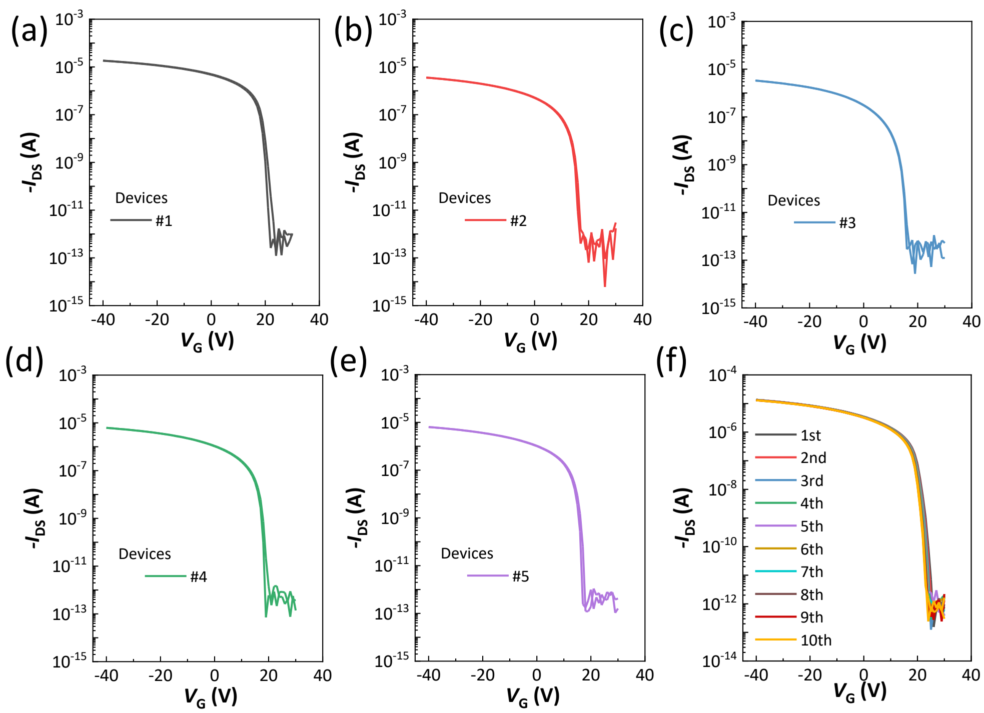

Fig. S9 (a-e) Hysteresis test of five SC-OFETs based on 2,6-DADTT; (f) multiple tests on one device.

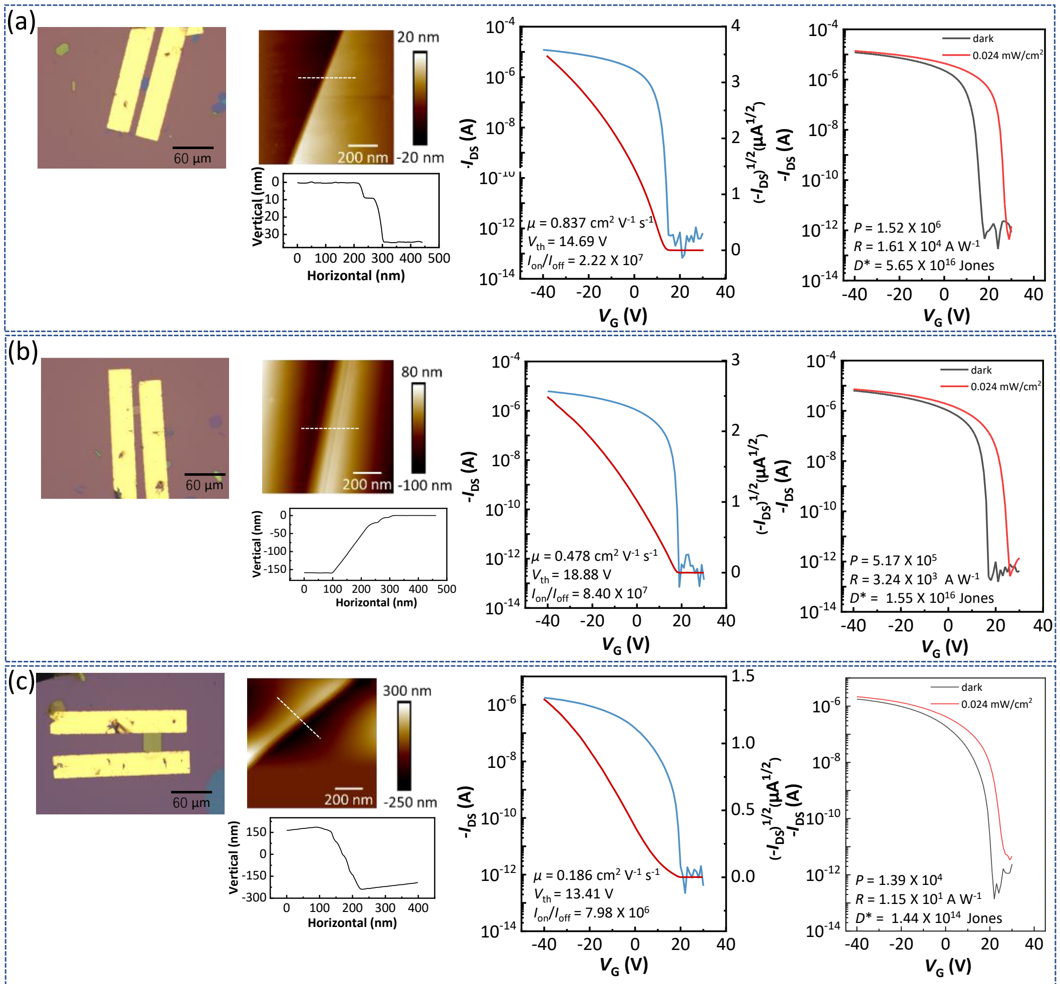

Fig. S10 Device performances based on 2,6-DADTT single crystal with different thickness (a, ~30 nm; b, ~150 nm; c, ~400 nm).

9. Characterization of 2,6-DADTT-based single crystal phototransistors.

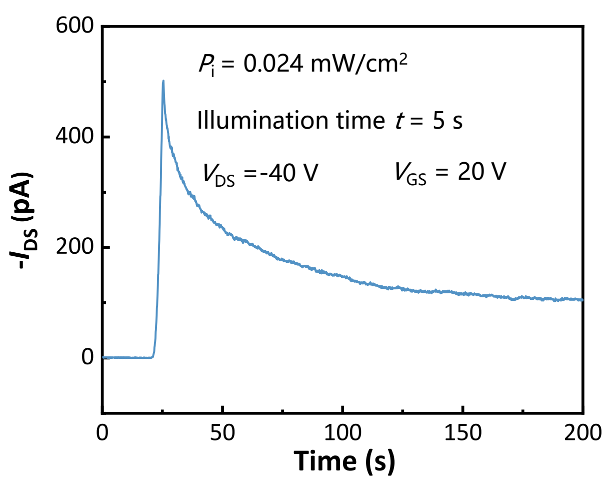

Fig. S11 The temporal response of 2,6-DADTT-based OPT.

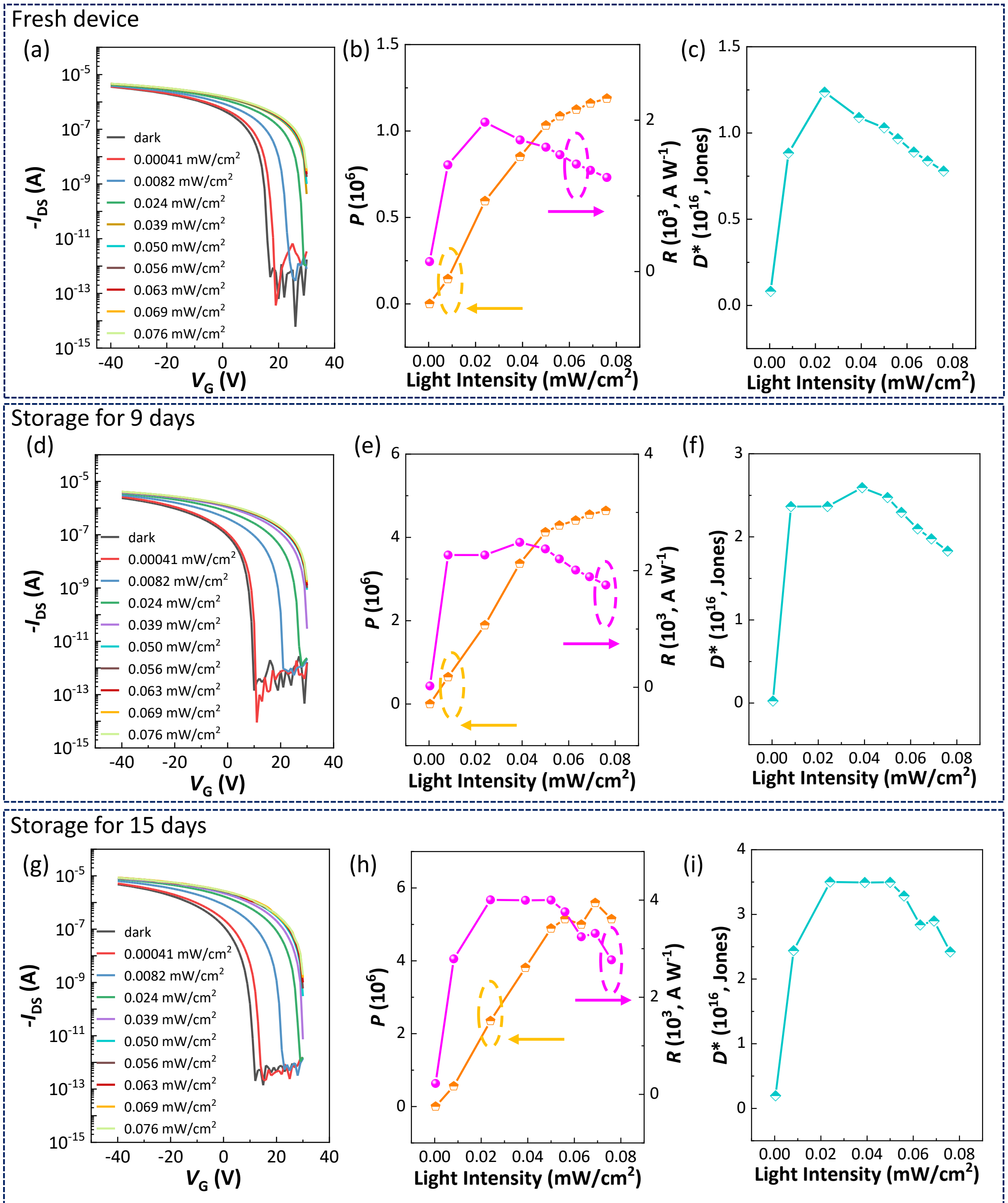

Fig. S12 Stability test of an 2,6-DADTT-based single crystal phototransistor. (a, d, g) Transfer curves of 2,6-DADTT-based OPT under various light intensity (365 nm). (b, e, h) *P*, *R* variation under different light intensity. (e, f, i) *D** variation under different light intensity.

10. MALDI-TOF MS

Analysis Info

Analysis Name	D:\Data\MALDI\2023\0103\LJ-1_0_I7_000003.d	Acquisition Date	1/3/2023 4:35:57 PM
Method	MALDI_P_100-3000	Operator	
Sample Name	MURU-N-ESI	Instrument	solariX
Comment			

Acquisition Parameter

Acquisition Mode	Single MS	Acquired Scans	2	Calibration Date	Fri Dec 16 05:39:37 2022
Polarity	Positive	No. of Cell Fills	1	Data Acquisition Size	2097152
Broadband Low Mass	202.1 m/z	No. of Laser Shots	10	Data Processing Size	4194304
Broadband High Mass	1000.0 m/z	Laser Power	17.4 lp	Apodization	Sine-Bell Multiplication
Source Accumulation	0.001 sec	Laser Shot Frequency	0.020 sec		
Ion Accumulation Time	0.010 sec				

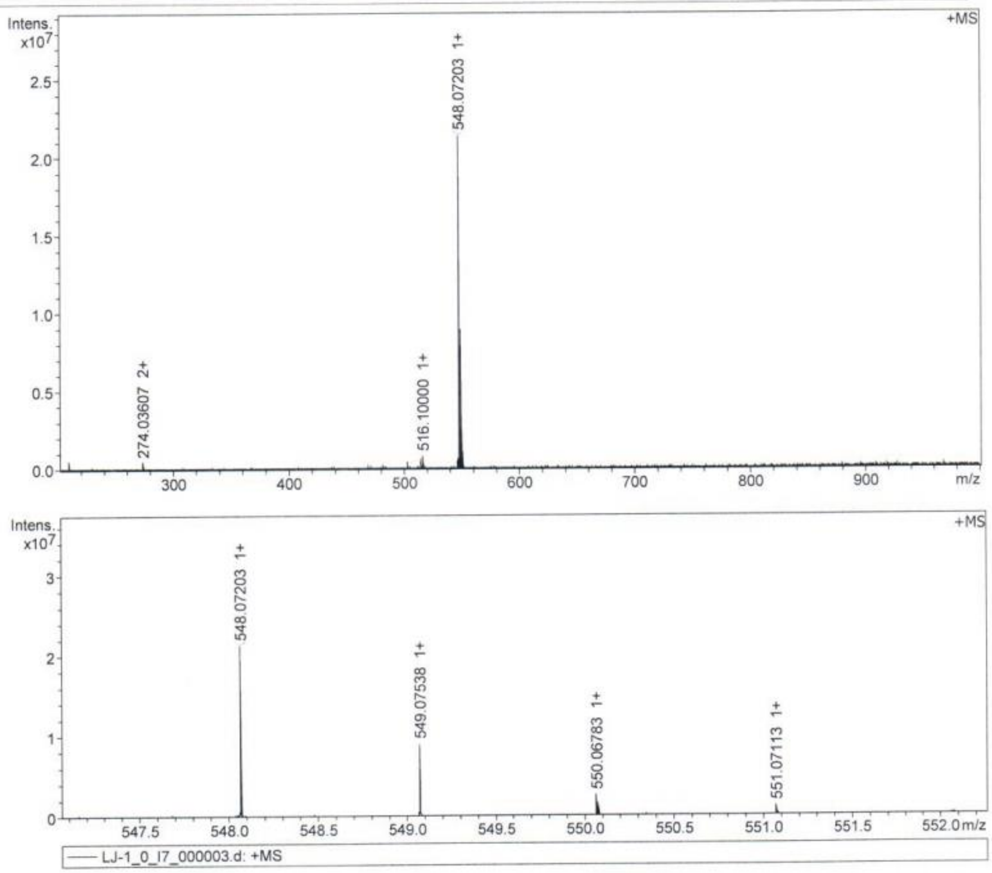

Meas. m/z	#	Ion Formula	Score	m/z	err [ppm]	Mean err [ppm]	mSigma	rdb	e⁻ Conf	N-Rule
548.072034	1	C36H20S3	100.00	548.072165	-0.2	0.1	90.6	27.0	odd	ok

11. Summary of the figures of merits of the UV-sensitive OPTs reported.

Table S4. Comparison of current work with representative UV-sensitive phototransistors based on organic semiconductors.

Semiconductors	Mobility ($cm^2 V^{-1} s^{-1}$)	Wavelength (nm)	Intensity ($\mu W cm^{-2}$)	*P*	*R* ($A W^{-1}$)	*D** (Jones)	Ref.
J-aggregated Anthracene derivative	0.40	400	1.4	$>10^4$	1.2×10^4	N/A	2
BBDTE	1.62	380	37	10^5	9821	N/A	3
BOPAnt	16.6	350	110	2×10^5	3.1×10^3	N/A	4
2-An-BTBT	0.9	380	17.7	1576	7136	N/A	5
1,6-DTEP	2.1	370	2.0	1.60×10^5	2.86×10^6	1.49×10^{18}	6
2,7-DTEP	0.025	370	2.0	4.35×10^3	1.04×10^5	5.28×10^{16}	
PY-4(THB)	0.7	400	5.6	1.2×10^6	2×10^4	N/A	7
C8-BTBT	1.57	365	200	3.0×10^4	1200	N/A	8
TPA-An	0.45	370	2.0	1.03×10^3	7.19×10^5	1.40×10^{16}	9
TBA-An	0.15	370	2.0	3.45×10^4	1.50×10^5	1.60×10^{17}	
2,6-DTEBDT	0.06	370	0.2	3.87×10^3	6.43×10^4	2.99×10^{16}	10
4,8-DTEBDT	0.25	370	0.2	7.36×10^4	9.60×10^5	5.68×10^{17}	
2,5-DATT	0.92	365	1.18	9×10^6	1.5×10^4	3×10^{15}	11
2,6-DADTT	1.26	365	35.5	2.49×10^6	6.84×10^3	4.70×10^{16}	This work

12. References

1. (a) Z. G. Shuai, Q. Peng, *Natl. Sci. Rev.* 2017, **4**, 224; (b) Q. Peng, Y. L. Niu, Q. H. Shi, X. Gao, Z. G. Shuai, *J. Chem. Theory Comput*. 2013, **9**, 1132; (c) Z. G. Shuai, *Chin. J. Chem*. 2020, **38**, 1223. (d) Z. G. Shuai, Q. Peng, *Phys. Rep*. 2014, **537**, 123.
2. H. Kim, S. Y. Bae, Y. S. Kim, J. A. Hur, M. H. Hoang, T. W. Lee, M. J. Cho, Y. Kim, M. Kim, J. Jin, S. J. Kim, K. Lee, S. J. Lee and D. H. Choi, *Adv. Mater.*, 2011, **23**, 3095–3099.
3. G. Y. Zhao, J. Liu, Q. Meng, D. Y. Ji, X. T. Zhang, Y. Zou, Y. G. Zhen, H. L. Dong and W. P. Hu, *Adv. Electron. Mater.*, 2015, **1**, 1500071.
4. A. Y. Li, L. J. Yan, M. Liu, I. Murtaza, C. He, D. W. Zhang, Y. W. Hea and H. Meng, *J. Mater. Chem. C*, 2017, **5**, 5304–5309.
5. L. J. Yan, M. W, Qi, A. Y. Li, H. Meng, X. Z. Zhao, M. U. Ali and B. M. Xu, *Org. Electron.*, 2019, **72**, 1–5.
6. J. W. Tao, D. Liu, Z. S. Qin, B. Shao, J. B. Jing, H. X. Li, H. L. Dong, B. Xu and W. J. Tian, *Adv. Mater.*, 2020, **32**, 1907791.
7. Y. S. Kim, S. Y. Bae, K. H. Kim, T. W. Lee, J. A Hur, M. H. Hoang, M. J. Cho, S. J. Kim, Y. Kim, M. Kim, K. Lee, S. Lee and D. H. Choi, *Chem. Commun.*, 2011, **47**, 8907–8909.
8. G. Wu, C. Chen, S. Liu, C. C. Fan, H. Y. Li and H. Z. Chen, *Adv. Electron. Mater.*, 2015, **1**, 1500136.
9. J. W. Tao, D. Liu, J. B. Jing, H. L. Dong, L. J. Liu, B. Xu and W. J. Tian, *Adv. Mater.*, 2021, **33**, 2105466.
10. J. W. Tao, Z. Y. Liu, D. Liu, H. L. Dong, J. B. Jing, J. X. Song, L. J. Liu, B. Xu and W. J. Tian, *Aggregate*., 2022, e269.
11. X. X. Yu, L. Zheng, J. F. Li, P. P. Yu, Z. Y. Liu, C. G. Li, Y. Zou, X. T. Zhang and W. P. Hu, *Org. Electron.*, 2020, **87**, 105941.